Journal of *Marine Science and Engineering*

MDPI

Article

Potential Effect of the Intrusion of the Kuroshio Current into the South China Sea on Catches of Japanese Eel (*Anguilla Japonica*) in the South China Sea and Taiwan Strait

Ching-Hsien Ho [1,*], Long-Jing Wu [2], Zhen Lu [3], Bo-Yi Lu [1] and Yang-Chi Lan [4]

[1] Department of Fisheries Production and Management, Sustainable Fisheries Development Research Center, National Kaohsiung University of Science and Technology, Kaohsiung 811, Taiwan; f109179104@nkust.edu.tw
[2] Ocean Conservation Administration, Ocean Affairs Council, Kaohsiung 806, Taiwan; 20031005@ntou.edu.tw
[3] Graduate School of Fisheries Sciences, Hokkaido University, Hakodate 041-8611, Japan; lvzhen2009@hotmail.com
[4] Coastal and Offshore Resource Research Center, Fisheries Research Institute, Council of Agriculture, Executive Yuan, Kaohsiung 806, Taiwan; yclan@mail.tfrin.gov.tw
* Correspondence: CCHO@nkust.edu.tw; Tel.: +886-7-3617141 (ext. #23514)

Abstract: This study examined the effect of the intrusion of the Kuroshio Current (KC) into the South China Sea (SCS) and the Taiwan Strait (TS) (SCS–TS region) on changes in catches of larval *A. japonica* in the traditional fishing ground waters of Gaoping near southwestern Taiwan in the SCS–TS region. First, the oceanic environment and recruitment trends from 1967 to 2019 were investigated based on secondary data. Then, field surveys were conducted to obtain primary data regarding the intrusion of the KC into the SCS, as well as the changes in the fishing sites and catches of *A. japonica* in the fall and winter of 2014–2015. Hence, the association between oceanic conditions and the number of *A. japonica* migrating into the SCS–TS region was explored. From 1967 to 2019, the recruitment proportion in the fishing grounds that formed due to the Kuroshio Branch Current (PKSBC) fluctuated significantly. Overall, positive values were observed for the Oceanic Niño Index for each year with a PKSBC > 50%, corresponding to El Niño conditions. In each year with a PKSBC > 70%, a looping path and a warm–core eddy appeared.

Keywords: Japanese eel; sea surface temperature anomaly; field study; Kuroshio Current; Kuroshio Branch Current; satellite remote sensing; environmental change; South China Sea; Taiwan Strait

Citation: Ho, C.-H.; Wu, L.-J.; Lu, Z.; Lu, B.-Y.; Lan, Y.-C. Potential Effect of the Intrusion of the Kuroshio Current into the South China Sea on Catches of Japanese Eel (*Anguilla Japonica*) in the South China Sea and Taiwan Strait. *J. Mar. Sci. Eng.* **2021**, *9*, 1465. https://doi.org/10.3390/jmse9121465

Academic Editor: Dariusz Kucharczyk

Received: 9 October 2021
Accepted: 14 December 2021
Published: 20 December 2021

1. Introduction

The Japanese eel *Anguilla japonica* is an important eel species for the marine fishery and aquaculture industries in East Asian countries and is currently the only eel species whose farming still relies on wild–caught larvae. Over the past three decades, environmental changes due to anthropogenic factors (e.g., deterioration and pollution of rivers and habitats, construction of reservoirs, and overfishing) coupled with climate change have led to a gradual depletion in larval eel stocks, which in turn has evoked a progressive decline in the offshore larval eel fishery industry. The catches of *A. japonica* began to decline for the first time in the 1970s [1]. Compared with the annual yield in the 1970s, the amount of *A. japonica* eels caught was 90% lower in 2016 [2]. Since 2010, the catches of *A. japonica* have declined by approximately 90% compared with the levels in 1960 [3,4]. However, intensifying climate change and accelerating decline in larval eel stocks may further increase the high volatility and uncertainty in catches of *A. japonica* from the fishing ground waters of Taiwan, which is where they migrate (including the Upstream Kuroshio and the South China sea (SCS)—Taiwan Strait (TS) region). In particular, these conditions may accelerate the decline in catches in the SCS–TS region, which is where the Kuroshio Branch Current (KSBC) intrudes [4].

The changes in oceanic circulation patterns and oceanic conditions may exacerbate the fluctuation in *A. japonica* stocks and the decline in *A. japonica* yields [4–8]. Through numerical simulations, many studies have demonstrated that the migration path of *A. japonica* is closely related to the intensity and location of the North Equatorial Current (NEC), Kuroshio Current (KC), KSBC, and Oceanic Niño Index (ONI). Changes in complex oceanic circulation patterns and climate regimes cause uncertainty and high volatility in the quality and number of migratory *A. japonica* [4,8,9]. The NEC, KC, and subtropical counter–current are the major ocean currents in the northwest Pacific that have undergone changes in recent decades compared with previously observed patterns [10–12]. For example, the KC has been warming approximately twice as fast as it did in the 19th century, with its main axis that extends to the East China Sea shifting gradually onshore [11,13]. As two other examples, the bifurcation of the NEC has begun to latitudinally shift southward over the past six decades, while the intensity of the KSBC extending from the Luzon Strait (LS) to the South China Sea (SCS) has gradually weakened over the past two decades [13,14]. These phenomena all suggest gradual changes in the oceanic circulation patterns in the northwest Pacific, as well as changes in oceanic migratory fish species (including *A. japonica*) in several aspects, namely, distribution patterns, migration paths, and numbers of fish that migrate, due to changes in ocean currents and oceanic conditions [4].

Located in the northeastern part of the SCS, the SCS–TS region, referring to the LS and the region to its west, is the main area through which the KSBC enters the SCS [15]. The physicochemical conditions of the ocean environment in this region are a convergence of complex ocean currents, including the KSBC, monsoon ocean currents, a cold eddy northwest of Luzon Island, and a warm–core eddy in the eastern part of the SCS, whose intensity varies seasonally and affects the quantity and geographical distribution of migratory fish in this region [16]. In winter, driven by northeasterly winds, the upper seawater of the KC bifurcates into two parts near 118° E, the main KC and the KSBC; the latter flows into the SCS through the waters of southern Taiwan and the LS (south of 20.25° N). This phenomenon is referred to as the intrusion of the KC [17]. Based on the collected absolute dynamic topography data, Nan et al. [15] identified three main types of paths along which the KSBC intrudes into the SCS: (1) leaping paths; (2) leaking paths; and (3) looping paths (the intrusion along this path can be further divided into two subphenomena: (A) type 3–A: looping path; and (B) type 3–B: on a type 3–A path, a cyclonic cold eddy circulation separates in the waters of the SCS) (Figure 1). Since 2000, changes in global oceanic circulation patterns have led to a gradual decline in both the frequency and intensity with which the KC intrudes into the SCS, which has resulted in a gradual decrease in the frequency at which a looping path occurs [13,15,16].

Over the past two decades, the formation of a looping path and a warm eddy in winter has been closely linked to the number of *A. japonica* that migrate to the SCS–TS region and has also been the primary factor affecting its catches [4,18]. According to the simulation results of high–resolution ocean models, only a few *A. japonica* entered the region north of 15° N each year after 2009 and were transported by the KC to the waters of East Asian countries compared with 1993–2008 [4,7]. Most of the larval *A. japonica* remained in the NEC region or were even transported southward. The decrease in the overall quantity of larval *A. japonica* transported to the waters of East Asian countries, the weakening of the intrusion of the KC, and the decrease in the frequency at which the KC intrudes into the SCS along a looping path have collectively led to a year–by–year decrease in the number of *A. japonica* transported by the KSBC into the SCS–TS region through the LS [4,7].

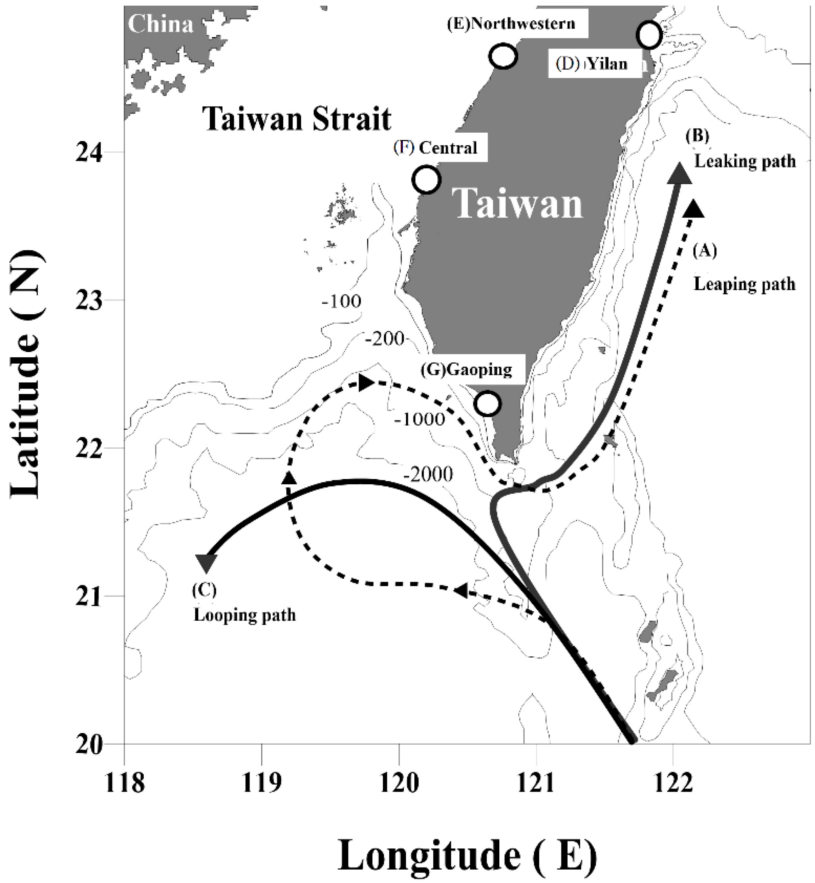

Figure 1. Types of paths along which the KC intrudes into the SCS–TS region and fishing ground locations of *A. japonica*. Three types of paths: (**A**) Looping path (left). (**B**) Leaping path (middle). (**C**) Leaking path (right). The location of four fishing grounds in Taiwan: (**D**) Yilan. (**E**) Northwestern. (**F**) Central. (**G**) Gaoping.

The evaluation results of high–resolution ocean models may have problems due to uncertainty with model accuracy in the absence of verification using in situ data [4,18–20]. Hence, this study was carried out for the following reasons:

(1) Determine the trend in oceanic environment characteristics, including the velocity and direction of the ocean currents, the sea surface temperature (TS), the Pacific Decadal Oscillation (PDO), the ONI, and recruitment from 1967 to 2019 based on secondary data;
(2) Investigate the trend of the KC intrusion into the SCS in the winter of 2014–2015 (i.e., between November 2014 and February 2015), as well as the changes in fishing sites and catches based on primary data acquired by a research test vessel (RTV) and a civilian fishing vessel (CFV) to determine the association between the changes in the oceanic conditions and the number of *A. japonica* migrating to the SCS–TS region; and
(3) Examine the association between the intrusion of the KC into the SCS and the TS (i.e., the SCS–TS region) and the changes in catches of larval *A. japonica* in the traditional fishing ground waters of Gaoping near southwestern Taiwan in the SCS–TS region.

Simultaneously, this study collected more in situ data and field survey data on the marine environment of the SCS–TS region and fishing operation conditions in the waters of Gaoping. We attempted to assist in solving the problem of in situ data from the SCS–TS region and hope that the results of this study can be used as a reference for other researchers.

2. Research Methods

To achieve these objectives, the oceanic environment and recruitment trends from 1967 to 2019 were investigated based on secondary data to understand the changes in the climate system and sea state change in the SCS–TS region under long–term trends. Then, field surveys were conducted to produce primary data, based on which the intrusion of the KC into the SCS as well as the changes in the fishing sites and catches of *A. japonica* in the fall and winter of 2014–2015 were examined. Thus, the association between the oceanic conditions and the number of *A. japonica* migrating into the SCS–TS region was explored. In terms of field surveys, a loaned RTV from the Fisheries Research Institute, Council of Agriculture, Executive Yuan, Taiwan, and a rental CFV were employed to survey and collect physicochemical conditions of the ocean environment and fishing data in the traditional fishing grounds for larval eels in the coastal waters of Gaoping (Figure 2).

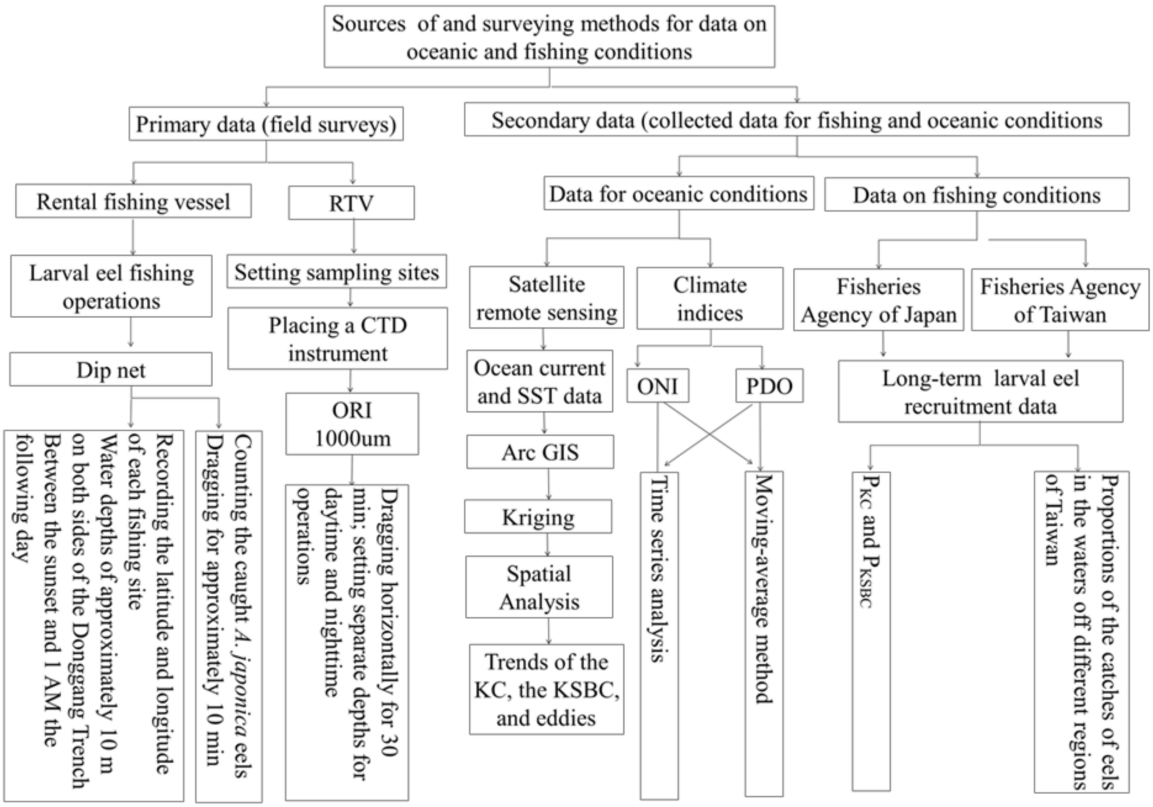

Figure 2. Research procedures and analytical methods used in this study.

2.1. Data for the Oceanic Environment, Fishing, Satellite

2.1.1. Climate Index Data (ONI and PDO)

Official National Oceanic and Atmospheric Administration (NOAA) data for the ONI and PDO from 1967 to 2019 were used in this study, accessed on 25 July 2021 (https://www.ncdc.noaa.gov/teleconnections/pdo/ and https://origin.cpc.ncep.noaa.gov/products/analysis_monitoring/ensostuff/ONI_v5.php (accessed on 25 October 2020)).

2.1.2. Fishing Data

Fall and winter (October through February of the following year) are the high seasons for catching *A. japonica* in the waters of Taiwan. *A. japonica* has been caught from the waters of both the main island of Taiwan and the Penghu Islands off the coast of Taiwan. Therefore, the larval eel catch data for Japan and Taiwan used in this study from fall and winter of 1967 to 2019 were retrieved from the Fisheries Agency, Ministry of Agriculture, Forestry and Fisheries of Japan and the AFSRT published by the Fisheries Agency of Taiwan

(accessed on 25 October 2020) (Statistics of Fishery Products in Japan [1], Annual Fishery Statistics Report of Taiwan (AFSRT) [2]).

2.1.3. Satellite Data

In terms of remote sensing data, the monthly SST data were sourced from the moderate resolution imaging spectroradiometer (MODIS) onboard the Aqua satellite launched by the National Aeronautics and Space Administration (NASA) for the region located at 116–122° E and 18–24° N from August 2003 to October 2019 (accessed on 25 May 2021).

The ocean current data sourced from the Copernicus Marine Environment Monitoring Service for the region located at 116–122° E and 18–24° N from December 1995, 2003, 2008, and 2014 (accessed on 25 July 2021).

2.2. Data Analysis Methods

2.2.1. ONI and PDO

NOAA's ONI is used to record historical occurrences and durations of El Niño episodes based on the monitoring of sea surface temperatures (SSTs) in the central Pacific Ocean. The ONI is used to identify the onset of an above–average SST threshold that persists for several months, encompassing both the beginning and end of an El Niño episode. The first appearance of an anomalous seasonal value of 0.5 °C suggests a high probability that an El Niño event could emerge [21]. The Pacific Decadal Oscillation (PDO) is often described as a long–lived El Niño–like pattern of Pacific climate variability. The PDO index is defined as the temporal coefficient of the leading EOF created from monthly SST anomalies poleward of 20°N in the Pacific basin; the positive and negative PDO indices represent the cooling and warming phases in the central Northwest Pacific [22,23]. This index is an interannual change in the distribution of *A. japonica* in the Northwest and North Pacific.

In this study, we used Excel 2019 to comprehensively arrange the values of monthly ONI and PDO from 1967 to 2019 and draw a long–term trend. We distinguished between the El Niño and La Niña periods based on the change trend periods of the positive and negative PDO and ONI values. In addition, to understand the influence and the relationship between the delayed effect of the climate system and catch change in KBSC, we selected several climate indices to perform Pearson regression analyses. The definitions of each climate index were ONI_Dec and PDO_Dec (the values of monthly ONI and PDO from December–February of the year before fishing operation), ONI_Jul and PDO_Jul (the values of monthly ONI and PDO from June–August of the six months before fishing operation), and ONI_DJF and PDO_DJF (the values of monthly ONI and PDO from December–February of the months on fishing operation).

2.2.2. Environmental Data

(1) Ocean Currents

The geostrophic current patterns were derived from satellite altimeter (0.25°–resolution) data from the December 1995, 2003, 2008, and 2014 were used in this study, accessed on 25 July 2021 (https://marine.copernicus.eu/).

(2) SST

Monthly SST data (spatial resolution: 4 km; unit: °C) acquired by MODIS onboard the Aqua satellite for the region located at 116–122° E and 18–24° N from August 2003 to October 2019 were used in this study (accessed on 25 May 2021), and we determined the monthly SST anomaly (SSTA) time series using the following equations:

$$\overline{SST}_m = \frac{\sum_{y=2003}^{2019} \overline{SST}_{ym}}{N} \quad (1)$$

$$SSTA_{ym} = \overline{SST}_{ym} - \overline{SST}_m \quad (2)$$

2.2.3. Spatial Statistics

Spatial statistics can help us to understand and evaluate the behaviour, trends, and patterns of change phenomena in the marine environment and help this study to summarize the distribution of several change phenomena from warm–core eddies in the waters of southwestern Taiwan to achieve the three objectives. Therefore, we used spatial statistics analyses in this paper, including tools for distribution analyses and spatial relationships. Spatial autocorrelation with global Moran's I and analyses of hot spots and kernel densities were performed for all SSTAs ($p < 0.05$) based on the Getis–OrdGi and kernel density functions [24]. Monthly MODIS SST data for the region located at 116–122° E and 18–24° N from November 2014 to February 2015 to cooperate with the in situ data results for the environmental survey and fishing operation period of 2014 to proceed with the discussion.

All spatial processing in this study was performed with ArcGIS 10.6 and its accessories. And positive and negative SSTAs in the SCS–TS region were calculated through spatial analyses in ArcGIS to determine the KC intrusion path and the mechanism behind the formation of the warm–core eddy in the SCS.

Based on the collected absolute dynamic topography data, the classification of Nan et al. [15] regarding the main types of paths along which the KSBC intrudes into the SCS was used: (1) leaping paths: the main KC does not bifurcate but rather flows directly towards the waters of eastern Taiwan after passing by the east side of Luzon Island. (2) Leaking paths: the KC bifurcates into two parts after passing by the northeastern corner of Luzon Island. One part continues to flow northward along the ocean ridges of Batan Island, while the other part turns northwestward and enters the SCS through the Balintang Channel. (3) Looping paths: the intrusion along this path can be further divided into two sub–phenomena: (A) Type 3–A: The KSBC enters the SCS along ocean ridges and generates a loop current after passing through the LS and then flows back to the path of the main KC. This path is referred to as a looping path. After entering the SCS, the KSBC rotates clockwise. (B) Type 3–B: On a type 3–A path, a cyclonic cold eddy circulation separates in the waters of the SCS.

2.2.4. Changes in the Catch Ratio between KC and KSBC

A. japonica has been caught from the waters off both the main island of Taiwan and the Penghu Islands off the coast of Taiwan. Of these waters, those in Yilan County and the town of Donggang, Pingtung County, Taiwan, produce relatively high yields [25,26]. Based on the formation mechanism, the traditional fishing grounds for larval eels of Taiwan can be categorized into two groups: (1) KC–induced fishing grounds and recruitment, including the waters of Yilan and northwestern Taiwan, and (2) KSBC–induced fishing grounds and recruitment, including the waters of Gaoping, central Taiwan, and the offshore islands of Taiwan (Figure 1). In this study, to determine the relationship between the intensity of the KC and KSBC and recruitment in different fishing grounds, the fishing grounds were first distinguished based on their two formation characteristics and then analysed separately to estimate their recruitment proportions (PKC + PKSBC = 100%, representing the proportion of recruitment in the fishing grounds that formed due to the KC and KSBC, respectively). To identify the cause of the changes in recruitment in the main KC and KSBC waters, we selected the year that had PKSBC > 70% from 1967–2019 in the SCS–TS region to examine the association between the intrusion of the KC into the SCS and the TS and the changes in catches of larval *A. japonica* in the traditional fishing ground waters of Gaoping near southwestern Taiwan, including December 1995, 2003, 2008, and 2014.

2.2.5. CFV–Borne Field Observations of Fishing Surveys

The Gaoping coast is an important traditional fishing ground for *A. japonica* in Taiwan (Figure 3A). Catches of *A. japonica* had a year change under the changes in KBSC influenced by the differences in the formation mechanism of the fishing ground (Figure 3B). Therefore, we selected Gaoping in the southwestern waters of Taiwan as the main survey area to collect in situ data to achieve objectives 2 and 3 (Figure 3).

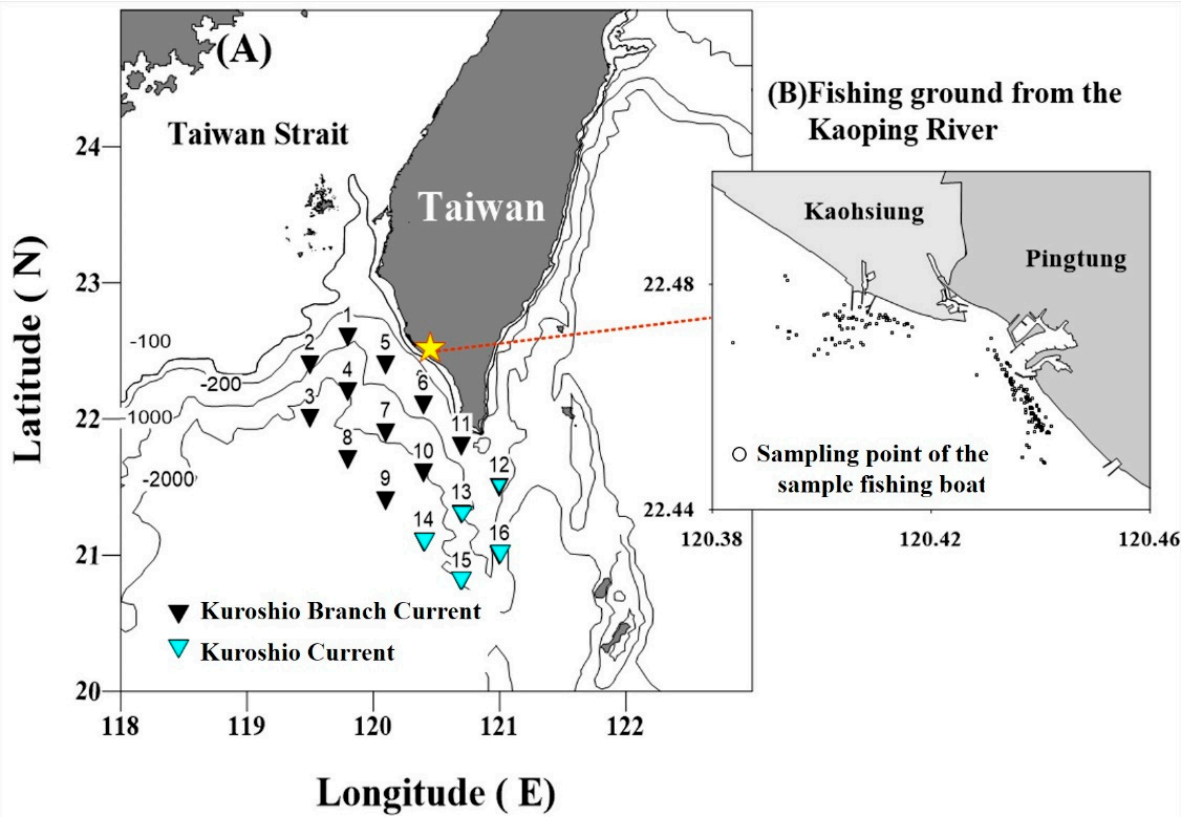

Figure 3. Locations of the shipborne sampling sites and sampling sites in the traditional fishing ground waters of Gaoping in southwestern Taiwan. (**A**) Locations of the shipborne sampling sites. (**B**) Sampling sites in the fishing sites of *A. Japonica*.

The traditional fishing grounds water of Gaoping off southwestern Taiwan are located at a depth of approximately 10 m near the estuary of the Gaoping River. Their shallow depth made it difficult to conduct surveys onboard the RTV. In this study, a CFV (specifically, a motor fishing raft) equipped with a dip net was rented to catch larval eels. Each survey lasted from before sunset (i.e., the time of departure from the port) to 1:00 a.m. the following day. At the start of each survey, the dip net was dragged for approximately 10 min, at which time we started to count the *A. japonica* caught and record the latitude and longitude of each fishing site. A total of four surveys on traditional fishing grounds were conducted between 2014 and 2015, specifically on 4–5 December 2014 (survey 1), 24–25 December 2014 (survey 2), 21–22 January 2015 (survey 3), and 27–28 January 2015 (survey 4) (Figure 3B).

Data regarding the physicochemical conditions of the ocean environment (thermohaline) were collected using a conductivity–temperature–depth instrument. During the test process, the instrument was lowered to a depth of 400 m to record the temperature and salinity of the seawater. Water sampling bottles were used to collect a 500–mL seawater sample from each of six zones located at depths of 0–5, 5–30, 30–50, 50–100, 100–200, and 200–300 m.

2.3. Correlation between KBSC Catches and Regional SST, PDO, and ONI

These climate indices are well documented and largely associated with the interannual variability in marine ecosystems and fisheries production in the Northwest and North Pacific [23,27]. The phenomenon of interannual change from El Niño and La Niña will cause the direction and velocity of KC and KSBC currents to change, and this change will lead to catch changes in the SCS–TS region. To achieve objectives 1 and 3, we used PDO, ONI, and catch data from 1967–2019 and regional SST from fall and winter from 2003–2019 in KSBC waters for Pearson correlation analyses to understand the possible impact of environmental changes on *A. japonica* catches. The independent variables were SST and

PDO with ONI, and the controlled variables were KBSC catch data. The analytical results were evaluated using Pearson's r and p values ($p < 0.05$ or <0.01 or <0.001), and divided into positive and negative correlations based on the results.

3. Results

3.1. Changes in the Global Climate Regime

3.1.1. Changes in the ONI

From 1967 to 2019, the ONI alternated between positive and negative values. The transition between El Niño and La Niña years can be roughly divided into several periods. The years 1968–1970 were El Niño years. From 1971 to 1976, La Niña conditions were largely observed, with only one interlude between 1972 and 1973, during which El Niño events occurred. Furthermore, 1995–1998 included El Niño conditions, followed by strong La Niña years between 1998 and 2001. Cumulative negative values were observed for the ONI during this period. Between 2002 and 2016, cumulative negative values were again observed for the ONI from 2007 to 2009 and 2010–2012, with cumulative positive values observed only from 2015 to 2016, suggesting El Niño conditions (Figure 4).

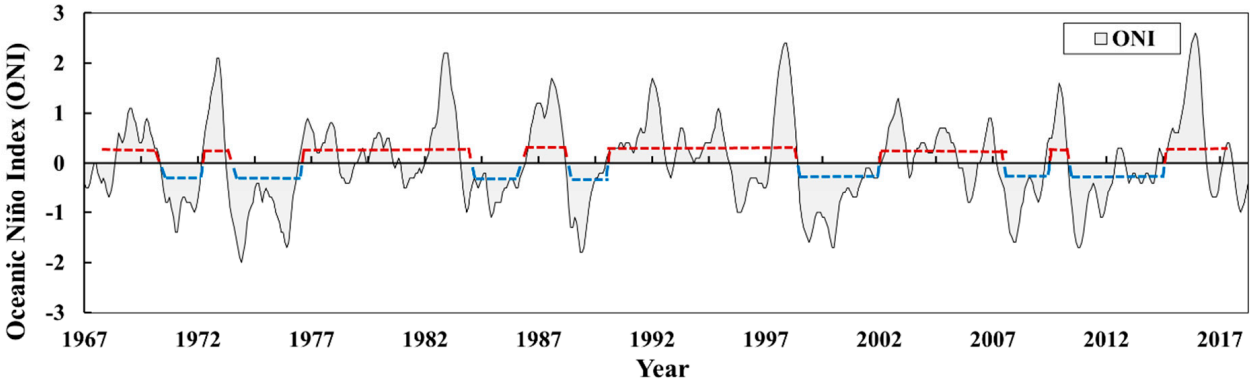

Figure 4. Trend in the ONI from 1967 to 2019. The data were obtained from NOAA, accessed on 25 May 2021 (http://origin.cpc.ncep.noaa.gov/products/analyses_monitoring/ensostuff/ONI_v5.php). The red dotted line is the El Niño period, and the blue dotted line is La Niña.

3.1.2. Changes in the PDO

Four stages of the PDO were observed from 1967 to 2019. The phase of the PDO was turned negative from 1967 to 1976, and turned positive again from 1977 to 1997, with cumulative positive values observed only from 1997, 1989 and 1995. This trend suggests that the waters of the west Pacific Ocean were relatively cold in this period. The phase of the PDO was largely negative from 1998 to 2013 and turned positive only from 2003 to 2007, indicating that the waters of the west Pacific Ocean were relatively warm after 1998. The phase of the PDO again turned from negative to positive in 2014 to 2019. Overall, the PDO alternated between positive and negative phases from 1967 to 2019 (Figure 5).

3.2. Changes in the Recruitment Proportions of Larval Eels in the Waters through Which the Main KC and KSBC Pass (Main KC Waters and KSBC Waters, Respectively)

The recruitment proportions in the waters of eastern, northeastern, central, and southern Taiwan and its offshore islands fluctuated considerably on an interannual scale from 1968 to 2019 (Figure 6). After dividing the *A. japonica* catch into PKC and PKSBC based on the fishing ground formation mechanism, we found that the catch proportion changed every year, and there was a phenomenon of regime change between PKC and PKSBC (Figure 7). In particular, PKSBC exceeded 50% in many years (i.e., 1968–1970, 1973–1974, 1986–1987, 1994–1996, 2002–2004, 2007–2008, and 2014) and even 70% in some years (e.g., 1995, 2003, 2008, and 2014) (please refer to Supplementary Materials). Analyses of the changes in PKC and PKSBC also revealed that waters with PKSBC > 70% were the primary supply source of *A. japonica* in each corresponding year.

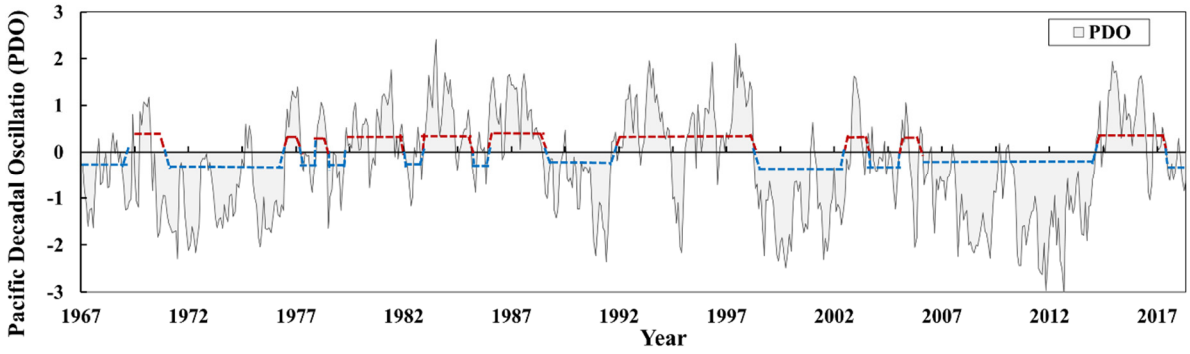

Figure 5. Trend in the PDO from 1967 to 2019. The data were obtained from NOAA, accessed on 25 May 2021 (http://www.esrl.noaa.gov/psd/data/climateindices/list/). The red dotted line is the warm water period, and the blue dotted line is the cold water period in the West Pacific.

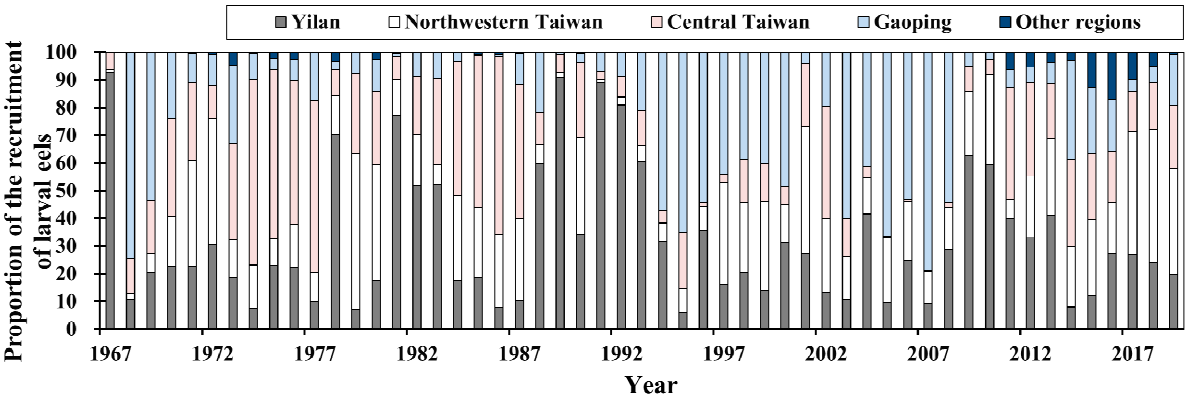

Figure 6. Trends in the recruitment proportions of larval eels in the waters of different regions of Taiwan from 1967 to 2019. The data were obtained from the AFSRT, accessed on 25 October 2020.

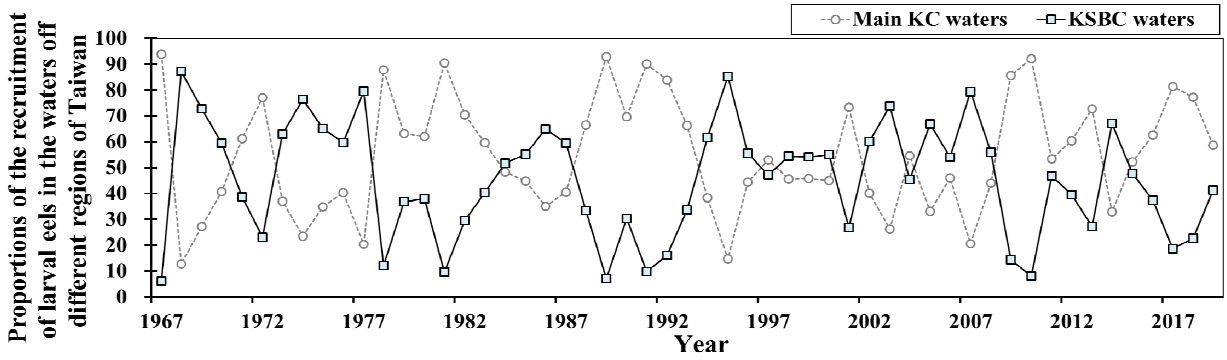

Figure 7. PKC and PKSBC from 1967 to 2019. The data were obtained from the (AFSRT), accessed on 25 October 2020.

3.3. Mesoscale Structural Changes in the Oceanic Environment in the SCS–TS Region

3.3.1. KC Intrusion and Looping Paths

Analyses of the distribution of the geostrophic velocity and direction of the KSBC in the waters of southwestern Taiwan revealed that the KC intruded into the SCS in December 1995, 2003, 2008, and 2014 (Figure 8). However, the KC took a looping path in December 2003, 2008, and 2014 (Figure 8B–D). Specifically, in each year, the KSBC entered the SCS along the ocean ridges after passing through the LS, forming a looping path, and then, it returned to the path of the main KC. Data analyses showed that the current velocity value was higher in the main KC and KSBC waters than in the surrounding sea waters, corresponding to a type 3–A path. After entering the SCS, the KSBC rotated clockwise in the waters between Dongsha and Taiwan, and its direction turned from northwest to north

and then to northeast and east, forming a circulation with a diameter of approximately 200 km in the open sea of Kaohsiung and Pingtung, Taiwan (Figure 8B).

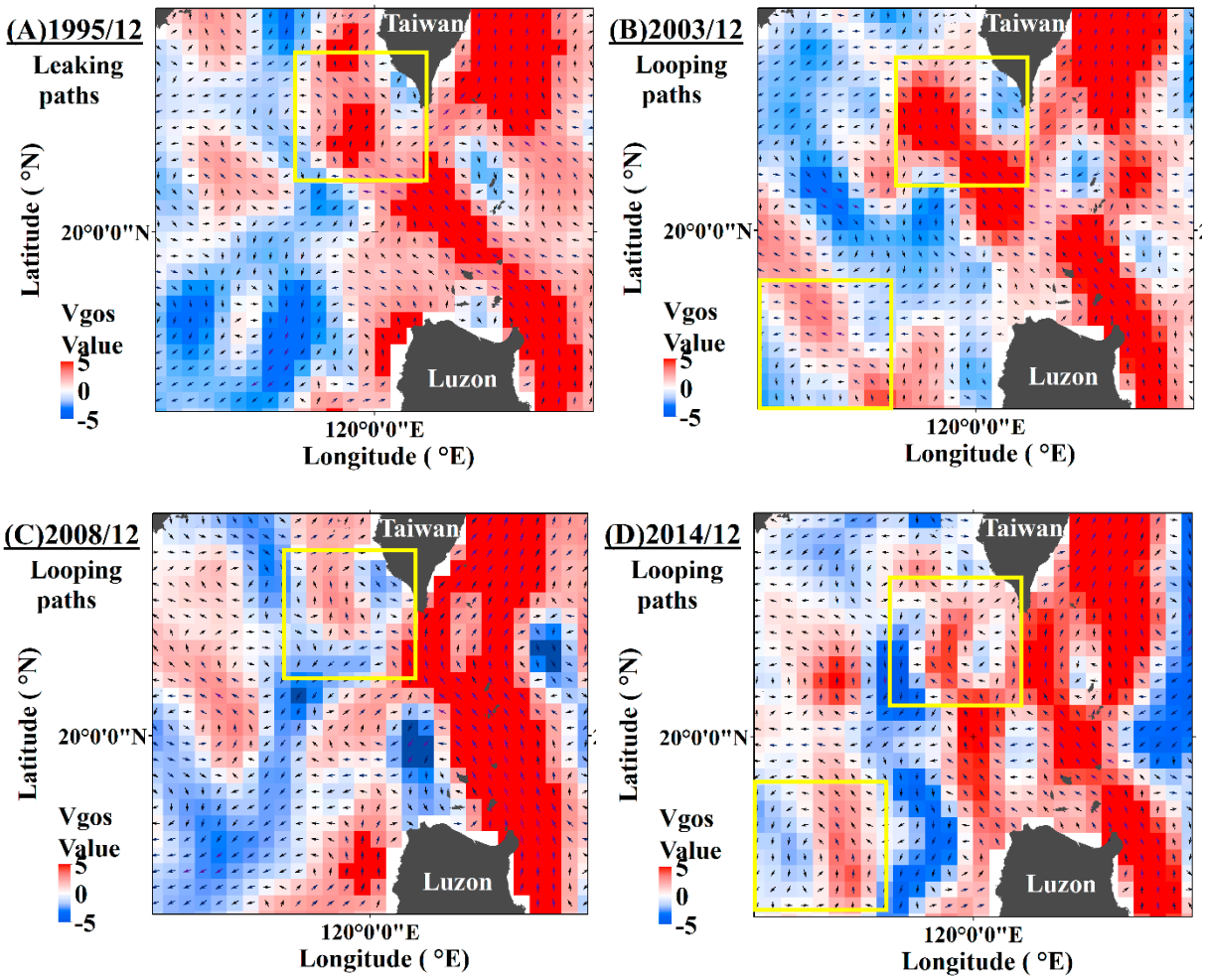

Figure 8. Distribution of the geostrophic velocity and direction of the KC during its intrusion into the waters of southwestern Taiwan in winter. (**A**) December 1995 (type of path: leaking path). (**B**) December 2003 (type of path: looping path (type 3–B)). (**C**) December 2008 (type of path: looping path (type 3–A)). (**D**) December 2014 (type of path: looping path (type 3–B)). The data were obtained from the Copernicus Marine Environment Monitoring Service. The yellow block in the figure is the geographical location by the looping paths (including type 3–A with 3–B).

3.3.2. Warm–Core Eddy in the Waters of Southwestern Taiwan

Analyses of the spatial distribution of the SSTAs and the edges of the KC between November 2014 and February 2015 showed the following characteristics. In November 2014, the KC had already bifurcated into two parts after passing by the northeastern corner of Luzon Island. The main KC continued to move northward along the ocean ridges of Batan Island, while the KSBC turned northwestward and entered the SCS through the Balintang Channel. A strong intrusion of the KC occurred. The main KC and KSBC waters were warmer than the adjacent waters (Figure 9A). In December 2014, a warm–core eddy that was warmer than the adjacent waters arose in the open sea of Kaohsiung and Pingtung, Taiwan, while a cold eddy that was colder than the adjacent waters appeared in the waters of the SCS, corresponding to a type 3–B path (Figure 9B). The intrusion of the KC continued into January 2015, which saw the disappearance of the warm–core eddy in the waters of southwestern Taiwan, weakening of the cold eddy in the SCS, and retreat of the edges of the KSBC (Figure 9C). In February 2015, the intrusion of the KC continued to weaken, with a continuous retreat of the edges of the KSBC, while the cold eddy in the SCS continued to decrease in both area and intensity (Figure 9D).

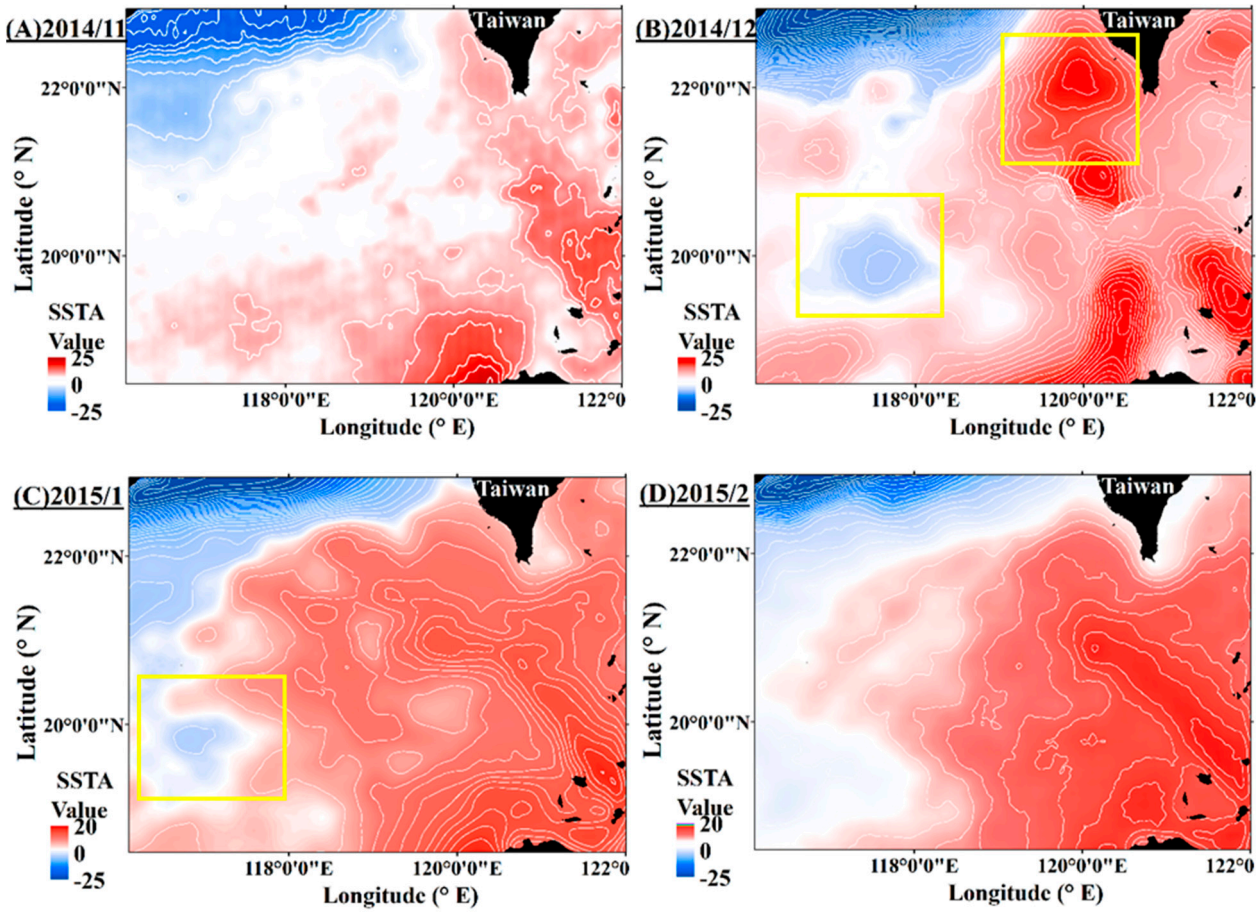

Figure 9. Spatial distribution of the positive and negative SSTAs in the waters of southwestern Taiwan in the fall and winter of 2014–2015 ($p < 0.05$). (**A**) November 2014. (**B**) December 2014. (**C**) January 2015. (**D**) February 2015. The data were obtained from MODIS onboard the Aqua satellite. The yellow block in the figure is geographical location by the warm core eddy in the SCS–TS region.

3.4. Field Survey Results

3.4.1. Changes in the Physicochemical Conditions of the Ocean Environment

The field surveys of the physicochemical conditions of the ocean environment conducted in 2014 yielded the following findings. In August, the SST was relatively high, at an average of 29.54 ± 0.17 °C, while the salinity of the seawater was 33.84 ± 0.56 practical salinity units (psu) (Figure 10A,B). In September, the average temperature and salinity of the seawater were 28.85 ± 0.79 °C and 33.55 ± 0.11 psu, respectively (Figure 10C).

Beginning in November, the thermohaline structure of the KC started to appear at sampling sites E13 and E14, while the thermohaline structure of the KSBC occurred at the other sampling sites. The average temperature and salinity of the seawater in November were 27.44 ± 0.44 °C and 34.32 ± 0.26 psu, respectively (Figure 10D). These results indicate the onset of an intrusion of the KC (Figure 10).

3.4.2. Changes in the Distribution of the Fishing Sites and *A. japonica* Catches

In November 2014, no *A. japonica* leptocephali were caught. Between 4 November 2014, and 28 January 2015, the dip net onboard the rental CFV was used to make 141 hauls at sea, catching a total of 211 leptocephali. During survey 1, 159 leptocephali were caught from 54 hauls made with the dip net onboard the rental CFV, primarily at sites 400 m offshore of the Gaoping River estuary in the open sea of Donggang (Figure 11A). Survey 2 produced fishing data for the open sea off both Kaohsiung and Pingtung. However, the catch (a total of 21 leptocephali from 21 hauls, averaging one eel per haul) obtained in survey 2 was smaller than that obtained in survey 1 (Figure 11B). The distribution of the

fishing sites of survey 3 was similar to that of survey 2. A total of 53 leptocephali were caught from 38 hauls in survey 3, averaging 0.62 eel per haul (Figure 11C).

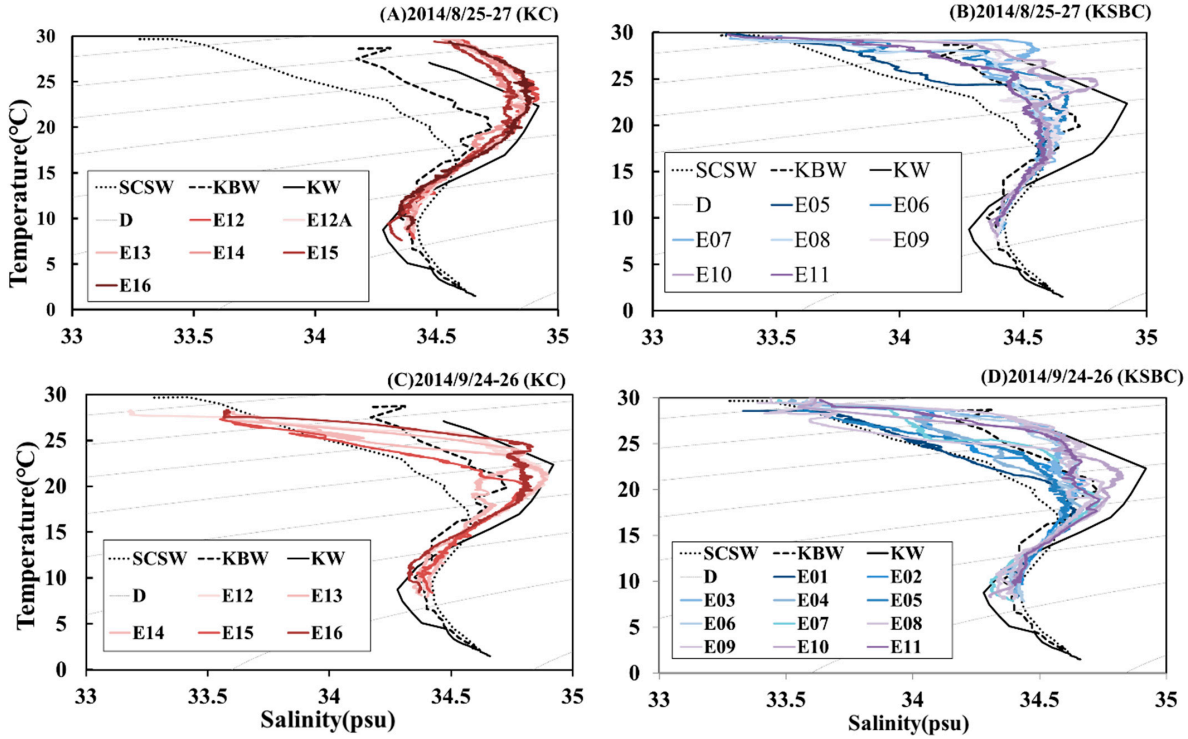

Figure 10. Changes in the ship–borne measurements of the surface temperature and salinity of the main KC and KSBC waters of southwestern Taiwan in 2014. (**A**) 25–27 August 2014 (KC). (**B**) 25–27 August 2014 (KSBC). (**C**) 24–26 September 2014 (KC). (**D**) 24–26 September 2014 (KSBC).

During survey 4, a total of 28 hauls were made in the open sea of Kaohsiung and Pingtung, with no catches of leptocephali (Figure 11D).

3.5. Correlation between Catches and ONI, PDO and Regional SST

The *A. japonica* catch changes were positively correlated with the changes in the ONI, PDO index, and regional SST in the KSBC according to the correlation statistics. Some indices exhibited no significant correlation. The correlation of the ONI_NDJ (December–February) with catches in the KSBC showed a significant positive correlation. The PDO_ Jul (June–August) index was significantly positively correlated with catches in the KSBC. The correlation coefficients of other factors were not significant (Table 1).

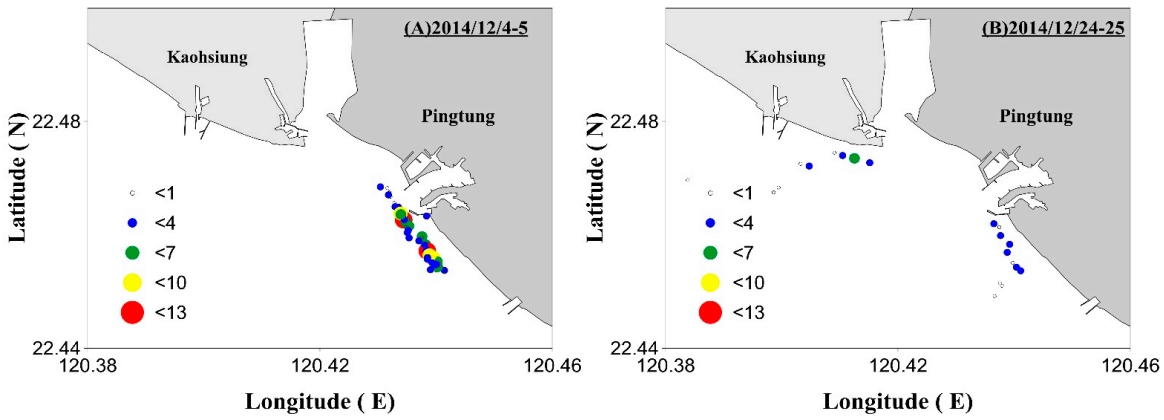

Figure 11. *Cont.*

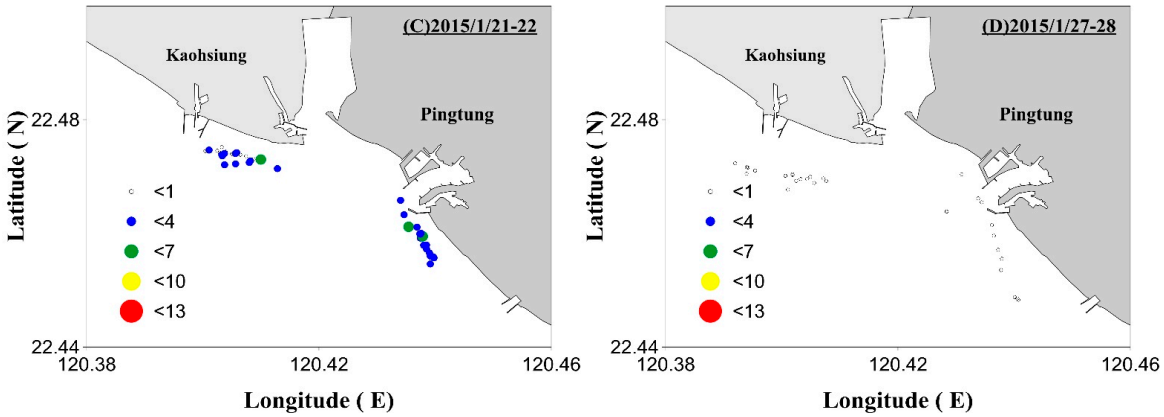

Figure 11. Locations and catches at the sampling sites of larval *A. japonica* eels. (**A**) 4–5 December 2014. (**B**) 24–25 December 2014. (**C**) 21–22 January 2015. (**D**) 27–28 January 2015.

Table 1. Pearson correlation between catches of *A. japonica* eels in the KSBC and regional SST, PDO, and ONI.

Climate and Environmental Index		Pearson's *r*	*p* Value
ONI	NDJ (December–February)	0.499 *	0.042
	JAS (June–August)	0.398	0.112
	DJF (December–February)	0.008	0.974
PDO	Dec (December–February)	0.339	0.183
	Jul (June–August)	0.500 *	0.038
	DJF (December–February)	0.125	0.634
SCS–TS Region		0.342	0.152

* $p < 0.05$.

4. Discussion and Conclusions

From 1967 to 2019, climate indices, such as the ONI and PDO, alternated between positive and negative values (Figures 4 and 5). Based on their transitions, this period can be divided into several subperiods, a pattern that suggests considerable changes in the climate regime and continual changes in the global oceanic environment in this 52–year period. Related research has examined the seasonal changes in and formation mechanisms of the surface circulations in the SCS using various methods, such as numerical models and satellite observations. Winds are the primary driver of changes in the circulations in the SCS. The waters of the northeastern SCS undergo more complex mesoscale changes and are also influenced by both the intrusion of the KC from the LS and the interannual variation in the driving action of winds [4]. By analysing the changes in the intrusion of the KC into the northeastern SCS in winter (December through February of the following year) through the results of satellite data and field data from this study (Figures 8–10), the KC intrusion mode is a key determiner of the formation of circulations and eddies, causing short–term changes and anomalies in the SST and sea surface height (Figure 9B,C).

In addition, the KC intrusion type may vary with time even during the same winter. Caruso et al. [17] found that the KC took a type 3–A looping path into the SCS in 1997, 1998, 1999, 2000, and 2003–2005; the type 3–A path turned into a type 3–B path in 1997, 1998, 1999, and 2003–2005; and the occurrence of a looping path was accompanied by the formation of an anticyclonic warm–core eddy in the open sea of Kaohsiung and a cyclonic cold eddy in the SCS. These findings are similar to the in situ data analyses in our study. Both the intensity and direction of the KSBC suggest that the KC intruded into the SCS along a looping path in December 2003, 2008, and 2014 (Figure 8B,D).

The spatial distribution maps of the ocean currents and SSTAs (Figures 8 and 9) reveal a strong intrusion of the KC into the SCS in the winter of 2014–2015. In November 2014, the warm water of the KC flowed northwestward through the LS and bifurcated near

121° E and 22° N (Figure 9A). The resulting KBSC continued to move northwestward. In December 2014, the KSBC intruded into the SCS near 118° E and 22° N. A portion of the KSBC seawater moved continuously westward, while its remaining seawater flowed southward along the coast of Taiwan, formed a loop, and then continued to the east. In addition, in December 2014, a warm–core eddy that was much warmer than the adjacent seawater appeared in the waters of southwestern Taiwan, while a cyclonic cold eddy was formed near 119.25° E and 21.5° N (Figure 9B). In January 2015, the warm–core eddy in the waters of Taiwan disappeared, while over time, the cold eddy in the SCS decreased gradually in both area and intensity under the constraint of the southwest current at the edge of the northwest continental shelf (Figure 9C). However, this phenomenon is consistent with the findings of Jan and Chao [28], Jan et al. [29], Nan et al. [16], and Caruso et al. [17] with respect to the intrusion of the KC and its path in the winter of 2002–2003. However, PKSBC exceeded 50% (Figure 7) (specifically, it was more than 70%) in each year when the KC intruded into the SCS along a type 3–A (Figure 8C) or 3–B looping path (Figure 8B,D). The *A. japonica* catch changes were positively correlated with the change trend in the ONI and PDO index in the KSBC according to the correlation statistics (Table 1). However, the correlation analyses also indicated that *A. japonica* catch changes were related to the KSBC intruding into the SCS and the interannual changes in ocean circulation.

The *A. japonica* fishing surveys in the winter of 2014–2015 yielded the following findings. Between November 2014 and February 2015, the distribution of the fishing sites and recruitment in the traditional fishing grounds of Gaoping shifted from south to north and gradually dispersed (Figure 11). In November 2014, even though observations confirmed that the high–temperature water of the KC had passed through the LS and that the KC intruded into the SCS, no *A. japonica* were caught during our fishing survey (Figures 9A and 11A). In December 2014, *A. japonica* began to be caught in the traditional fishing grounds of Gaoping, which were located primarily in the open sea of Pingtung. Recruitment was relatively densely distributed (Figure 11B). In January 2015, the fishing sites in the fishing grounds began to spread out, which was accompanied by a decrease in recruitment (Figure 11C). In February 2015, no *A. japonica* leptocephali were caught on our fishing survey (Figure 11D). Instead, *A. japonica* leptocephali began to be caught in the fishing grounds in the waters of northern Taiwan, where the main KC passed [2].

By simulating the number of larval *A. japonica* migrating between the Mariana Trench and the northwest Pacific, Chang et al. [4] found a considerable decrease in the number of *A. japonica* in the waters of Japan and Taiwan in the past two decades, which they mostly attributed to the decrease in the intensity of the KC. From 1994 to 2012, the number of larval *A. japonica* in the SCS–TS region decreased at an annual rate of approximately 8.2%, faster than those in the other seven (e.g., the Pacific Subtropical Counter–current region, the East China Sea, and the waters of southern Japan) of the eight major sea regions to which *A. japonica* migrated. Changes in the global climate regime are a factor causing changes in the recruitment of *A. japonica* (Figures 8 and 9). The Pearson correlation results of this study also show that changes in the global climate system may affect the *A. japonica* catches in the SCS–TS region. From the field observation data in 2014 (PKSBC > 70%), it was also found that the fluctuation trend in recruitment in the traditional fishing grounds of Gaoping was similar to the intrusion trend of the KC in winter as well as the trends of the warm–core eddy along the coast of Taiwan and the cold eddy in the SCS (Figure 9).

To provide in situ field data for the sea state and fishing conditions of the SCS–TS region of *A. japonica*, we investigated the trend of the KC intrusion into the SCS in the winter of 2014–2015 as well as the changes in fishing sites and catches based on primary data acquired by an RTV and a CFV to determine the association between the changes in oceanic conditions and the number of *A. japonica* migrating to the SCS–TS region. However, the possible influencing factors of the distribution and resource changes in *A. japonica* are very diverse, including the population dynamics, environmental conditions during the spawning season, and so on. These factors may possibly affect the population run of

A. japonica. Furthermore, the changes in *A. japonica* stocks are affected by several factors, both natural/environmental and anthropogenic [28,29]. However, the consequences of global warming and changes in the climate regime, such as weakening of seasonal atmospheric circulations and equatorial trade winds, affect the distribution and migration of eels worldwide [4,18–20]. Therefore, more in–depth analyses and observations are required to more accurately identify the association between the changes in the ocean current patterns caused by global climate regime changes and the fishing grounds and conditions for eels in the future.

Supplementary Materials: The following are available online at https://www.mdpi.com/article/10.3390/jmse9121465/s1. *A. japonica* catch proportions data for Taiwan from 1967 to 2019.

Author Contributions: Conceptualization, C.-H.H. and L.-J.W.; methodology, C.-H.H. and Z.L.; software, C.-H.H. and B.-Y.L.; investigation, Y.-C.L.; writing—original draft preparation, C.-H.H.; writing—review and editing, C.-H.H.; project administration, L.-J.W.; funding acquisition, C.-H.H. and L.-J.W. All authors have read and agreed to the published version of the manuscript.

Funding: This research was funded by the National Science Council of the Republic of China [Taiwan) and Council of Agriculture, Executive Yuan (Taiwan), grant numbers (MOST 110–2621–M–865 –001 –, [MOST 110–2621–M–992–001 –] and [110–A.T–13.1.1-F–A1].

Acknowledgments: We thank the anonymous reviewers and the editor of the journal for their comments and suggestions.

Conflicts of Interest: The authors declare that they have no conflicts of interest. The funders had no role in the design of the study; in the collection, analyses, or interpretation of data; in the writing of the manuscript; or in the decision to publish the results.

Abbreviations

AFSRT	Annual Fishery Statistics Report of Taiwan	ONI	Oceanic Niño Index
CFV	Civilian Fishing Vessel	PDO	Pacific Decadal Oscillation
KC	Kuroshio Current	PKC	Proportion of Kuroshio Current
KSBC	Kuroshio Branch Current	PKSBC	Proportion of Kuroshio Branch Current
LS	Luzon Strait	RTV	Research Test Vessel
MODIS	Moderate Resolution Imaging Spectroradiometer	SCS	South China Sea
NASA	National Aeronautics and Space Administration	SST	Sea Surface Temperature
NEC	North Equatorial Current	SSTA	Sea Surface Temperature Anomaly
NOAA	National Oceanic and Atmospheric Administration	TS	Taiwan Strait

References

1. Fisheries, Statistics of Fishery Products in Japan. Available online: http://www.maff.go.jp/j/tokei/kouhyou/kensaku/bunya6.html (accessed on 25 October 2020).
2. Annual Fishery Statistics Report of Taiwan. Available online: https://www.fa.gov.tw/cht/PublicationsFishYear/index.aspx (accessed on 25 October 2020).
3. ICES. *Report of the Joint EIFAAC/ICES Working Group on Eels (WGEEL), 18–22 March 2013 in Sukarietta, Spain, 4–10 September 2013 in Copenhagen, Denmark*; ICES: Copenhagen, Denmark, 2013; Volume 18, p. 851.
4. Chang, Y.-L.; Miyazawa, K.Y.; Miller, M.J.; Tsukamoto, K. Potential impact of ocean circulation on the declining Japanese eel catches. *Sci. Rep.* **2018**, *8*, 5496. [CrossRef]
5. Friedland, K.D.; Miller, M.J.; Knights, B. Oceanic changes in the Sargasso Sea and declines in recruitment of the European eel. *ICES J. Mar. Sci.* **2007**, *64*, 519–530. [CrossRef]
6. Zenimoto, K.; Sasai, Y.; Sasaki, H.; Kimura, S. Estimation of larval duration in Anguilla spp., based on cohort analysis, otolith microstructure, and Lagrangian simulations. *Mar. Ecol. Prog. Ser.* **2011**, *438*, 219–228. [CrossRef]
7. Chang, Y.-L.; Sheng, J.; Ohashi, K.; Béguer-Pon, M.; Miyazawa, Y. Impacts of Interannual Ocean Circulation Variability on Japanese Eel Larval Migration in the Western North Pacific Ocean. *PLoS ONE* **2015**, *10*, e0144423. [CrossRef]
8. Hsu, A.C.; Xue, H.; Chai, F.; Xiu, P.; Han, Y.-S. Variability of the Pacific North Equatorial Current and its implications on Japanese eel (Anguilla japonica) larval migration. *Fish. Oceanogr.* **2017**, *26*, 251–267. [CrossRef]
9. Tsukamoto, K. Oceanic migration and spawning of anguillid eels. *J. Fish Biol.* **2009**, *74*, 1833–1852. [CrossRef]

10. IPCC. *Climate Change 2014: Synthesis Report*; Contribution of Working Groups I, II and III to the Fifth Assessment Report of the Intergovernmental Panel on Climate Change; IPCC Press: Geneva, Switzerland, 2014; pp. 1–151, ISBN 97892-91691432.
11. Ho, C.H.; Lu, H.J.; He, J.S.; Lan, K.W.; Chen, J.L. Changes in Patterns of Seasonality Shown by Migratory Fish under Global Warming: Evidence from Catch Data of Taiwan's Coastal Fisheries. *Sustainability* **2016**, *8*, 273. [CrossRef]
12. Peyser, C.E.; Yin, J.; Landerer, F.W.; Cole, J.E. Pacific Sea level rise patterns and global surface temperature variability. *Geophys. Res. Lett.* **2016**, *43*, 8662–8669. [CrossRef]
13. Wu, C.R.; Wang, Y.L.; Lin, Y.F.; Chao, S.Y. Intrusion of the Kuroshio into the South and East China Seas. *Sci. Rep.* **2017**, *7*, 7895. [CrossRef]
14. Chen, Z.; Wu, L. Long-term change of the Pacific North Equatorial Current bifurcation in SODA. *J. Geophys. Res. Ocean.* **2012**, *117*, C6. [CrossRef]
15. Nan, F.; Xue, H.; Chai, F.; Shi, L.; Shi, M.; Guo, P. Identification of different types of Kuroshio intrusion into the South China Sea. *Ocean Dyn.* **2011**, *61*, 1291–1304. [CrossRef]
16. Nan, F.; Xue, H.; Yu, F. Kuroshio intrusion into the South China Sea: A review. *Prog. Oceanogr.* **2015**, *137*, 314–333. [CrossRef]
17. Caruso, M.J.; Gawarkiewicz, G.G.; Beardsley, R.C. Interannual variability of the Kuroshio intrusion in the South China Sea. *J. Oceanogr.* **2006**, *62*, 559–575. [CrossRef]
18. Han, Y.S.; Lin, Y.F.; Wu, C.R.; Iizuka, Y.; Castillo, T.R.; Yambot, I.U.; Mamalangkap, M.D.; Yambot, A.V. Biogeographic distribution of the eel Anguilla luzonensis: Dependence upon larval duration and oceanic currents. *Mar. Ecol. Prog. Ser.* **2016**, *551*, 227–238. [CrossRef]
19. Baltazar-Soares, M.; Biastoch, A.; Harrod, C.; Hanel, R.; Marohn, L.; Prigge, E.; Evans, D.; Bodles, K.; Behrens, E.; Böning, C.; et al. Recruitment Collapse and Population Structure of the European Eel Shaped by Local Ocean Current Dynamics. *Curr. Biol.* **2014**, *24*, 104–108. [CrossRef]
20. Naisbett-Jones, L.C.; Putman, N.F.; Stephenson, J.F.; Ladak, S.; Young, K.A. A Magnetic Map Leads Juvenile European Eels to the Gulf Stream. *Curr. Biol.* **2017**, *27*, 1236–1240. [CrossRef]
21. Glantz, M.H.; Ramírez, I.J. Reviewing the Oceanic Niño Index (ONI) to Enhance Societal Readiness for El Niño's Impacts. *Int. J. Disaster Risk Sci.* **2020**, *11*, 394–403. [CrossRef]
22. Mantua, N.J.; Hare, S.R. The pacific decadal oscillation. *J. Oceanogr.* **2002**, *58*, 35–44. [CrossRef]
23. Tian, Y.J.; Kidokoro, H.; Watanabe, T. Long-term changes in the fish community structure from the Tsushima warm current region of the Japan/East Sea with an emphasis on the impacts of fishing and climate regime shift over the last four decades. *Prog. Oceanogr.* **2006**, *68*, 217–237. [CrossRef]
24. Aghajani, M.A.; Dezfoulian, R.S.; Arjroody, A.R.; Rezaei, M. Applying GIS to Identify the Spatial and Temporal Patterns of Road Accidents Using Spatial Statistics (case study: Ilam Province, Iran). *Transp. Res. Procedia* **2017**, *25*, 2126–2138. [CrossRef]
25. Tzeng, W.N.; Cheng, P.W.; Lin, F.Y. Relative abundance, sex ratio and population structure of the Japanese eel Anguilla japonica in the Tanshui River system of northern Taiwan. *J. Fish Biol.* **1995**, *46*, 183–200. [CrossRef]
26. Tzeng, W.-N.; Tabeta, O. First record of the short-finned eel Anguilla-bicolor-pacifica elvers from Taiwan. *Bull. Japan. Soc. Sci. Fish.* **1983**, *49*, 27–32. [CrossRef]
27. Beamish, R.J.; McFarlane, G.A.; King, J.R. Fisheries climatology: Understanding decadal scale processes that naturally regulate British Columbia fish populations. In *Fisheries Oceanography: An Integrative Approach to Fisheries Ecology and Management*; Blackwell Scientific Publications: Oxford, UK, 2000; pp. 94–139.
28. Jan, S.; Chao, S.Y. Seasonal variation of volume transport in the major inflow region of the Taiwan Strait: The Penghu Channel. *Deep-Sea Res. Part II-Top. Stud. Oceanogr.* **2003**, *50*, 1117–1126. [CrossRef]
29. Jan, S.; Wang, J.; Chern, C.-S.; Chao, S.-Y. Seasonal variation of the circulation in the Taiwan Strait. *J. Mar. Syst.* **2002**, *35*, 249–268. [CrossRef]